

## Article

# Laboratory Investigation and Machine Learning Modeling of Road Pavement Asphalt Mixtures Prepared with Construction and Demolition Waste and RAP

Fabio Rondinella <sup>1</sup>, Cristina Oreto <sup>2</sup>, Francesco Abbondati <sup>3</sup> and Nicola Baldo <sup>1,\*</sup>

<sup>1</sup> Polytechnic Department of Engineering and Architecture (DPIA), University of Udine, Via del Cottonificio 114, 33100 Udine, Italy; fabio.rondinella@uniud.it

<sup>2</sup> Department of Civil, Construction and Environmental Engineering (DICEA), Federico II University of Naples, 80125 Naples, Italy; cristina.oreto@unina.it

<sup>3</sup> Department of Engineering, University of Naples Parthenope, 80143 Naples, Italy; francesco.abbondati@uniparthenope.it

\* Correspondence: nicola.baldo@uniud.it

**Abstract:** Due to the decreasing availability of virgin materials coupled with an increased awareness of environmental sustainability issues, many researchers have focused their efforts on investigating innovative technological solutions in the civil engineering domain. This paper aims to evaluate the suitability of construction and demolition waste (C and DW) and reclaimed asphalt pavement (RAP) reused within asphalt mixtures (AMs) prepared for the binder layer of road pavements. Both hot and cold mixing methodologies were investigated. The technical assessment was based on the volumetric and mechanical suitability, according to saturated surface dry voids (SSDV) and indirect tensile strength (ITS) tests carried out at 10 °C, respectively. Laboratory findings showed that all the hot AMs matched the desired target SSDV at the design gyrations number at different optimum bitumen content levels, alternatively showing a non-significant variation or a significant increase in ITS compared to conventional hot mix asphalt. Conversely, the cold AMs with cement and emulsion bitumen showed a greater volume of voids and moisture sensitivity, and lower temperature susceptibility compared to hot AMs, reaching, on average, 11% lower ITS when using coarse C and DW aggregates and 43% lower ITS when using filler from C and DW. These volumetric and mechanical properties were modeled by means of support vector machines and categorical boosting (CatBoost) machine learning algorithms. The results proved to be satisfactory, with CatBoost determination coefficients  $R^2$  referring to SSDV and ITS equal to 0.8678 and 0.9916, respectively. This allowed for the mechanical performance of these sustainable mixtures to be predicted with high accuracy and implemented within conventional mix design procedures.

**Keywords:** road pavement; asphalt mixtures; construction and demolition waste; RAP; machine learning; support vector machine; categorical boosting



**Citation:** Rondinella, F.; Oreto, C.; Abbondati, F.; Baldo, N. Laboratory Investigation and Machine Learning Modeling of Road Pavement Asphalt Mixtures Prepared with Construction and Demolition Waste and RAP.

*Sustainability* **2023**, *15*, 16337.

<https://doi.org/10.3390/su152316337>

Academic Editor: Edoardo Bocci

Received: 31 October 2023

Revised: 24 November 2023

Accepted: 24 November 2023

Published: 27 November 2023



**Copyright:** © 2023 by the authors. Licensee MDPI, Basel, Switzerland. This article is an open access article distributed under the terms and conditions of the Creative Commons Attribution (CC BY) license (<https://creativecommons.org/licenses/by/4.0/>).

## 1. Introduction

In 2015, the United Nations announced 17 sustainable development goals (SDGs) to focus the attention of all member states on several economic, environmental, and sustainability issues [1,2]. In particular, the 9th SDG is related to the topics of resilient infrastructure building, sustainable industrialization, and resource consumption reduction [3]. Achieving these goals is not only interesting from a technical feasibility perspective, but also extremely important to successfully reach the transition towards the circular economy planned for 2030 [4,5].

Within this framework, the road pavement construction field has always been particularly sensitive to sustainability issues, and for many years researchers have devoted their efforts to the reuse of so-called secondary raw materials [6–11]. Increasingly cutting-edge technological solutions have been developed to allow for end-of-life materials and

industrial by-products to be properly recycled in the production of asphalt mixtures (AMs). Nevertheless, technical considerations must always be made to evaluate the mechanical performance of the end-of-life materials and industrial by-products used to prepare sustainable AMs [12].

By way of example, polyethylene waste plastic was investigated in both high-density and low-density forms. The former proved to be suitable as a binder modifier, decreasing permanent deformation [13,14]. On the other hand, the latter allowed for AMs to be more resistant to rutting phenomena [15]. With the aim of achieving the so-called “zero waste” goal [16], electric arc furnace steel slags have been investigated over the years as a substitute for natural aggregate. These have not only shown chemical and physical characteristics fully consistent with their intended purposes but also provide suitable mechanical performance, reduce water damage and consequently improve durability both in asphalt- and cement-bound mixtures [17].

With the aim of further improving the sustainability of the produced AMs, innovative procedures related to the predictive modeling of their mechanical behavior have been also investigated in the last decades [18–21]. In fact, being able to know in advance the volumetric properties or the mechanical behavior of asphalt mixtures based on a few compositional variables can provide several advantages. By way of example, (i) the estimation of parameters that need to be used within the traditional road pavement design procedures can be considerably faster and more accurate; and (ii) both time and money required to prepare additional samples for testing can be saved, limiting the consumption of additional raw materials and waste production [22].

As a result, many researchers have begun to explore several alternatives for predictive methodologies. Empirical ad hoc equations, as well as constitutive equations, have been developed over the years [23–26]. More recently, machine learning (ML) models have been designed to identify reliable relationships between analyzed variables and provide even more accurate predictions [27–36]. Two of the well-established ML algorithms implemented in these methodologies are related to support vector machines (SVMs) and decision trees (DTs); the former were proposed by Vapnik [37] and are able to accomplish supervised learning tasks. They have found many interesting applications within the asphalt pavement field by successfully predicting the international roughness index [38], or the icing phenomenon and its influencing factors [39]. The latter have been deeply explored in their boosting variants, namely LightGBM [40], XGBoost [41] and CatBoost [42], for the prediction of the rutting depth of asphalt concrete containing reclaimed asphalt pavement (RAP) [43].

The main goals of the present study can be contextualized within this framework since they deal with: (i) the investigation of both hot and cold asphalt mixing technologies, to evaluate if suitable mechanical performance can be achieved while also lowering the mixing temperatures; (ii) the possibility of reusing waste materials like construction and demolition waste (C and DW) in different sizes and RAPs that would otherwise be disposed of in landfills, without significantly affecting the main volumetric and mechanical parameters that the mixtures should meet to actually be used to build road pavements; and (iii) performance modeling using several ML algorithms.

To achieve these goals, an extensive experimental campaign was carried out on several mixtures prepared for the binder course layer of road pavements with both hot and cold mixing technologies using C and DW and RAP as a partial replacement for primary materials like limestone aggregates and limestone filler. The indirect tensile strength (ITS) at 10 °C was evaluated to determine the mechanical suitability of these sustainable mixtures. Subsequently, laboratory results were processed by means of SVM and CatBoost algorithms to develop an ML methodology for the prediction of the mixtures’ volumetric properties and mechanical behavior.

The paper is therefore structured as follows: Section 2 outlines a detailed description of the materials analyzed, the testing procedures, the resulting dataset, and the main soft-computing techniques investigated. Section 3 describes the results obtained from both

the experimental campaign and the machine learning modeling, comparing the goodness-of-fit metrics achieved by each developed model and focusing the attention on the best-performing one. A sensitivity analysis was then carried out to get a deeper comprehension of the resulting predictions. Finally, Section 4 provides the main conclusions that can be drawn from the present study, pointing out its limitations and aspects that will need further investigation with future developments.

## 2. Materials and Methods

### 2.1. Asphalt Mixtures

The object of the present study is the mechanical investigation of 7 alternative AMs, produced using both hot and cold mixing technologies and different secondary raw materials contents, for the binder layer of road pavements.

Asphalt mixtures are produced by mixing mineral aggregates with asphalt-based binders. In the present study, different limestone products, namely 3 coarse aggregate sizes (3/6 mm, 6/12 mm and 10/20 mm), a limestone sand (0/4 mm) and a limestone filler, were used; the secondary raw materials introduced in the asphalt mixtures as a substitute for natural ones were the reclaimed asphalt pavement (RAP), with a size designation, according to UNI EN 13108-8 [44], of U RA 0/8, and construction and demolition waste (C and DW) sampled from a recycling facility in the form of a coarse aggregate, namely, C and DW1 (2/16 mm), and a filler (C and DW2).

All the aggregates underwent a preliminary characterization to assess their compliance with the main Italian technical specifications for road pavement binder layers [45] in terms of: (a) Los Angeles value (UNI EN 1097-2) [46] and flattening index (UNI EN 933-3) [47] measured on all aggregates with sizes greater than 4 mm, which were lower than 25% and 15, respectively, for all the aggregates analyzed; and (b) the sand equivalent value (UNI EN 933-8) [48], measured on all aggregates with sizes below 4 mm, which was always lower than the threshold value of 60%.

For the asphalt binders, a commercial 50/70 penetration-grade neat bitumen and a hard modified bitumen PMB 10/40–70, obtained through the addition of 5% SBS polymer to a 70/100 penetration-grade neat bitumen, were adopted to produce the hot mix asphalts. A Portland cement 325R and an over-stabilized bitumen emulsion (made up of 40% water and 60% bitumen modified with an SBS polymer) were used in the mix design of the cold recycled solutions.

The 7 investigated asphalt mixtures are as follows:

- HMAMod as the conventional hot mix asphalt with 100% limestone aggregates and an SBS polymer-modified bitumen (9 observations);
- HMAc and DW1 as the hot mix asphalt with neat bitumen 50/70, where 40% of the limestone aggregates are substituted with construction and demolition waste aggregates (C and DW1) (6 observations);
- HMAModC and DW1 as the hot mix asphalt with modified bitumen, where 40% of the limestone aggregate is substituted with construction and demolition waste aggregates (C and DW1) (9 observations);
- CMA as the conventional cold mix asphalt with 76% RAP and limestone aggregates mixed with bitumen emulsion, cement, water, and additives (9 observations);
- CMAC and DW1 as the cold mix asphalt with 30% RAP, construction and demolition waste aggregates (C and DW1) and limestone aggregates mixed with bitumen emulsion, cement, water, and additives (9 observations);
- CMAC and DW2\_1 as the cold mix asphalt with 76% RAP, 4% filler from construction and demolition waste (C and DW2) and limestone aggregates mixed with bitumen emulsion, cement, water, and additives (10 observations);
- CMAC and DW2\_2 as the cold mix asphalts with 30% RAP, 6% filler from construction and demolition waste (C and DW2) and limestone aggregates mixed with bitumen emulsion, cement, water, and additives (18 observations).

For the hot asphalt mixtures, given the aggregate composition that meets the main Italian technical specifications for the grading curve of the asphalt mixtures for the binder layer of road pavements [45], 3 specimens were compacted using a gyratory compactor for the final number of gyrations for each trial bitumen content, until these reached the target saturated surface dry voids (SSDV), equal to 4%, determined experimentally and calculated according to the design number of gyrations specified by EN 12697-6 [49] and EN 12697-8 [50]. After proper conditioning at the 10 °C test temperature, the same specimen underwent ITS testing (EN 12697-23) [51] to check the maximum tensile stress at failure arising in the diametral plane of a cylindrical specimen due to compressive loading.

For the cold mix asphalts, a similar procedure was applied with some major differences, as follows: (a) the object of the mix design is the emulsion bitumen content that minimizes air voids, while the optimum content of water and cement in each mixture has been mostly defined upstream of the mix design process to maximize the dry density of the mixture of aggregates bonded with cement and water; and (b) the specimens are conditioned in an oven at 40 °C for 72 h to allow for curing before measuring the air voids and ITS.

## 2.2. Database Description

The goal of this section is to provide both qualitative and quantitative descriptions of the 11 analyzed variables that will later be involved in the design of machine learning models. These descriptions will also be useful in understanding the applicability limitations of the developed models and defining their improvement potential.

The distribution of the sampled points with respect to the measured values of indirect tensile strength at 10 °C can be observed in Figure 1. In each subplot, the  $y$ -axis shows the corresponding value of ITS while the  $x$ -axis shows the value of the following investigated variables: the gyratory revolutions (GR); construction and demolition waste contents (C and DW1 and C and DW2); reclaimed asphalt pavement (RAP); water content (WC); cement content (CC); emulsion bitumen content (EBC); total bitumen content (TBC, sum of the fresh bitumen, bitumen in the emulsion and rejuvenated bitumen in the RAP); and saturated surface dry voids (SSDV). It can be seen that each point on the graphs is associated with a different color depending on the corresponding mixing technology used (identified by means of a categorical variable). Furthermore, equally colored histograms are shown to provide insight into the number of observations for each category.

A statistical description of the investigated variables is provided in Table 1. Thus, the unit of measurement, the total number of observations, and the respective minimum, maximum, mean, and standard deviation values are reported. Modeling efforts will be subsequently aimed at identifying machine learning algorithms capable of accurately and reliably predicting ITS values at 10 °C and SSDV solely based on the mixing technology, the number of gyratory revolutions, and all the percentage contents of secondary raw materials, water, cement, and bitumen. In this way, the investigated mixtures can be characterized both from volumetric and mechanical points of view, allowing for the predictions to be used within the conventional mix design procedures for road pavement construction.

The Pearson correlation matrix based on the analyzed dataset is shown in Figure 2. For the subsequent modeling operations, it is important to observe that the SSDV showed a strong positive correlation with the RAP percentage ( $R = +0.84$ ), highlighting the high value of the relationship's strength and a direct proportionality between them. On the other hand, ITS at 10 °C showed several strong negative correlations with EBC ( $R = -0.88$ ), WC ( $R = -0.79$ ), CC ( $R = -0.73$ ), and RAP ( $R = -0.72$ ).

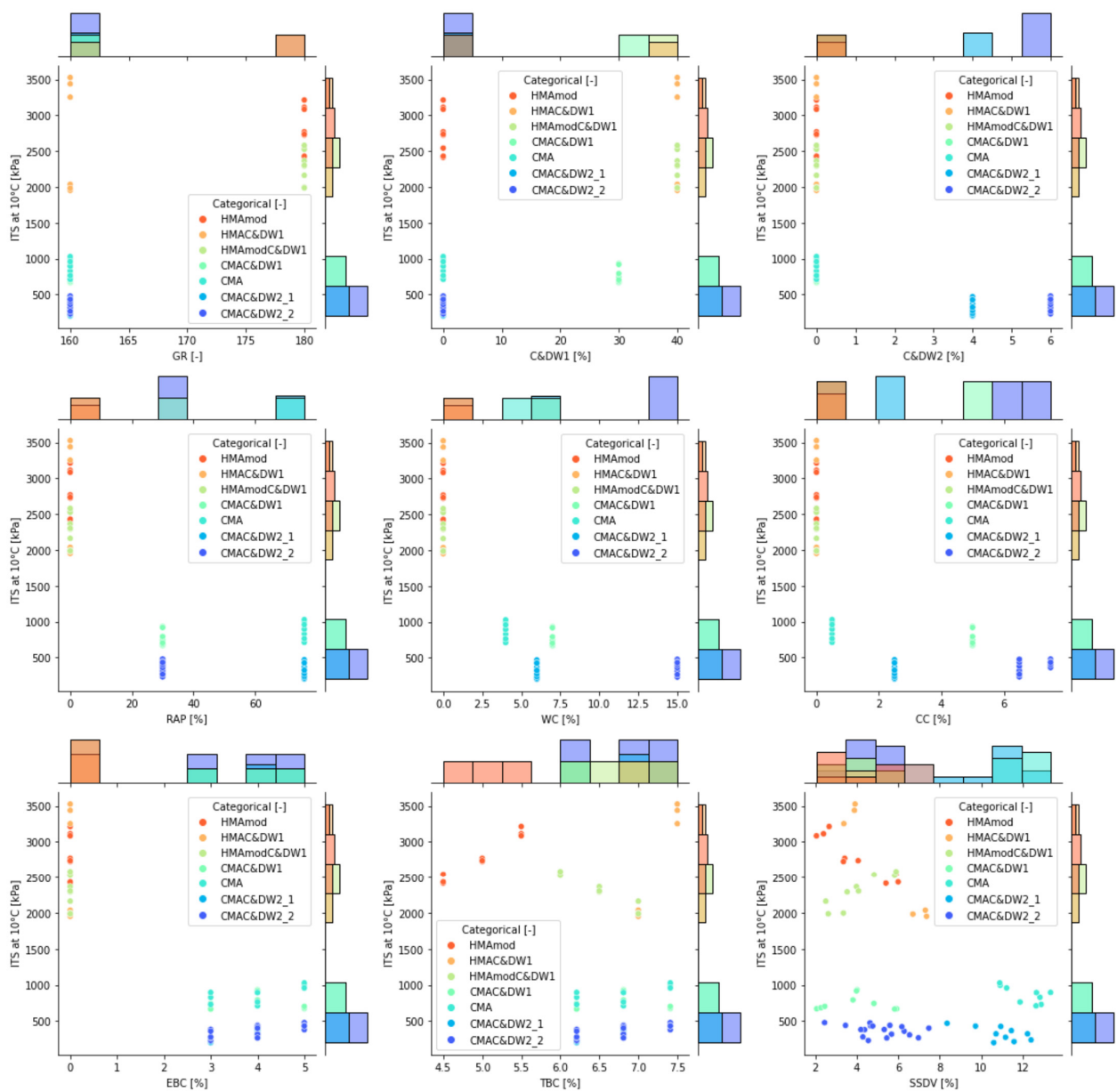
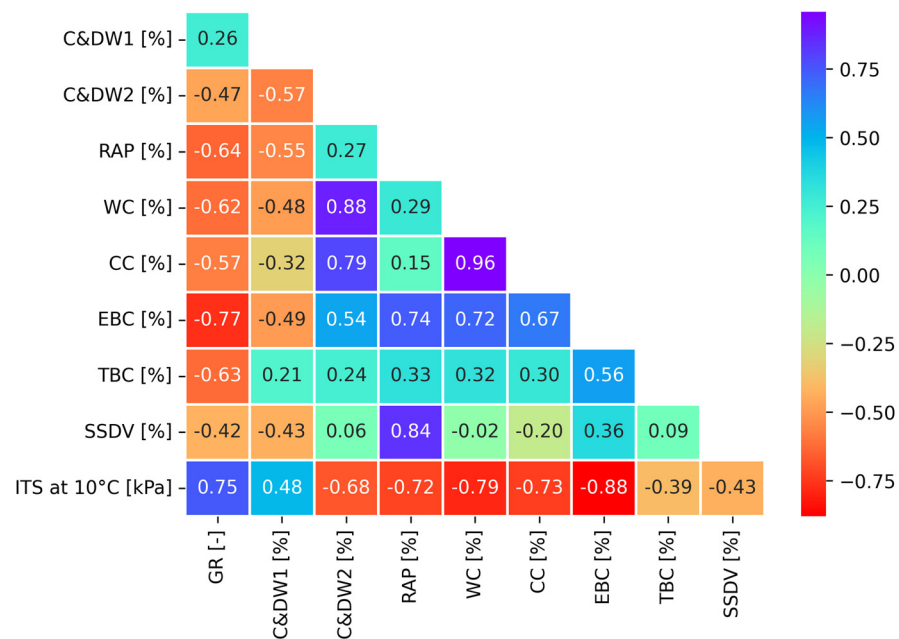


Figure 1. Data distribution between ITS at 10 °C and all the considered variables.

Table 1. Statistical description of the analyzed variables.

Variable	Description	U.M.	Min <sup>1</sup>	Max <sup>1</sup>	Average <sup>1</sup>	Std Dev <sup>1</sup>
Categorical	Mixing Technology	—	—	—	—	—
GR	Gyratory Revolutions	—	160.00	180.00	165.14	8.80
C and DW1	Construction and Demolition Waste Aggregates Content	%	0.00	40.00	12.43	17.56
C and DW2	Construction and Demolition Waste Filler Content	%	0.00	6.00	2.11	2.68
RAP	Reclaimed Asphalt Pavement Content	%	0.00	76.00	32.20	29.85
WC	Water Content	%	0.00	15.00	6.13	5.85
CC	Cement Content	%	0.00	7.50	2.86	2.95
EBC	Emulsion Bitumen Content	%	0.00	5.00	2.63	2.02
TBC	Total Bitumen Content	%	4.50	7.50	6.57	0.78
SSDV	Saturated Surface Dry Voids	%	2.06	13.35	6.48	3.42
ITS at 10 °C	Indirect Tensile Strength at 10 °C	kPa	202.08	3529.01	1237.25	1036.81

<sup>1</sup> Descriptive statistic is based on 70 observations.



**Figure 2.** Strength of Pearson correlation between analyzed variables.

### 2.3. Support Vector Machine Modeling

Support vector machines (SVMs) represent supervised machine learning methodologies that are remarkably suited to addressing both classification (SVC) and regression (SVR) tasks, even in the presence of a limited dataset size and high dimensionality problems [52]. SVMs are widely used in pavement engineering and have been successfully implemented in recent years for different predictive modeling purposes [39,53].

The main goal of an SVR is to identify the hyperplane  $f(x)$  that, based on the loss function  $L$ , maximizes the margin  $\epsilon$  accounting not only for the predictive error, but also for the model generalization capabilities determined according to the trade-off parameter  $C$ .

Root mean squared error (RMSE) was implemented as the loss function, and its mathematical formulation is reported in Equation (1):

$$RSME = \sqrt{\frac{1}{n} \sum_{i=1}^n (y_{T_i} - y_{P_i})^2} \quad (1)$$

where subscripts  $T$  and  $P$  stand for targets and predictions, respectively.

Given a dataset  $D = \{(x_i, y_i), i = 1, 2, \dots, n\}$ , where  $x_i$  represents the feature vector in the input space and  $y_i$  represents the corresponding target value, the mathematical framework of an SVR model can be described as shown in Equations (2) and (3):

$$f(x) = \omega^T \varphi(x) + b \quad (2)$$

$$L_\epsilon(f(x_i) - y_i) = \begin{cases} 0 & \text{if } |f(x_i) - y_i| \leq \epsilon \\ |f(x_i) - y_i| - \epsilon & \text{if } |f(x_i) - y_i| > \epsilon \end{cases} \quad (3)$$

Assuming that the experimental observations are not linearly separable in the original space, it is common practice to apply a transformation  $K(x_i, x_j)$  that maps the starting data into a higher dimensional feature space. Such a procedure is called the kernel method, and the most frequently used transformations are linear (Lin), polynomial (Poly), radial basis function (RBF), and sigmoidal (Sigm) [54]. These were implemented in the present study and are mathematically described in Equations (4)–(7):

$$K(x_i, x_j) = x_i^T x_j \quad (4)$$

$$K(x_i, x_j) = \left(-\gamma \cdot x_i^T x_j + 1\right)^d \quad (5)$$

$$K(x_i, x_j) = \exp\left(-\gamma \|x_i - x_j\|^2\right) \quad (6)$$

$$K(x_i, x_j) = \tanh\left(-\gamma \cdot x_i^T x_j + 1\right)^d \quad (7)$$

$C, \gamma, d$  and the transformation function represent important hyperparameters that can be properly optimized.

#### 2.4. CatBoost Modeling

An innovative decision-tree-based supervised ML algorithm to accomplish both classification and regression tasks was proposed in 2017 by Prokhorenkova et al. [42]. It was called CatBoost and, as suggested by the name, combined a gradient-boosting algorithm with the capability of handling categorical features. It consists of an ensemble method that obtains a strong learner based on the combination of multiple weak base learners, usually represented by decision trees [55].

Assuming that the dataset can be again summarized as  $D = \{(x_i, y_i), i = 1, 2, \dots, n\}$ , the goal of the supervised learning process is to identify a function  $F(x)$  so that the expected loss  $L(F) := \mathbb{E}L(y, F(x))$  is minimized. A standard gradient-boosting algorithm iteratively updates the function  $F(x)$  and can be mathematically summarized as follows, in (Equations (8) and (9)):

$$F^{t+1} = F^t + \alpha \cdot h^{t+1} \quad t = 0, 1, \dots \quad (8)$$

$$h^{t+1} = \underset{h \in H}{\operatorname{argmin}} L(F^t + h) = \underset{h \in H}{\operatorname{argmin}} \mathbb{E}L(y, F^t(x) + h(x)) \quad (9)$$

where  $\alpha$  and  $h^{t+1}$  represent the learning step size and a weak base predictor, respectively.

Defining  $-g^t(x, y) := \frac{\partial L(y, s)}{\partial s} \Big|_{s=F^t(x)}$ ,  $h^{t+1}$  can then be expressed as shown in Equation (10):

$$h^{t+1} = \underset{h \in H}{\operatorname{argmin}} \mathbb{E}(-g^t(x, y) - h(x))^2 \quad (10)$$

For a comprehensive overview of the entire algorithm, please refer to the research proposed by Prokhorenkova et al. [42]. CatBoost was developed to successfully address two main issues related to the functioning of the conventional gradient-boosting algorithm, namely, prediction shift and target leakage [42]. The advantages of using CatBoost rather than other traditional implementations of gradient-boosting can be summarized as follows: (i) base learners consist of decision tables (also called level-wise symmetric trees) [56–58] that use the same split criterion for each level; (ii) ordered boosting replaces traditional methods for residuals evaluation and subsequent gradient estimation; (iii) random permutation is performed to randomly arrange samples during the ordered boosting; (iv) categorical features can be automatically handled by means of one-hot encoding, which converts them into target statistics. The resulting tree architecture is more balanced and allows for faster evaluations during the testing phase, reducing the occurrence of overfitting [59].

Since multiple simultaneous predictions are allowed while using the CatBoost algorithm, MultiRMSE was selected in this case as the loss function (Equation (11)):

$$\text{MultiRMSE} = \sqrt{\frac{1}{N} \sum_{i=1}^N \sum_{d=1}^D (y_{T_{i,d}} - y_{P_{i,d}})^2} \quad (11)$$

where  $D$  represents the total number of output variables.

### 2.5. Algorithm Optimization

For modeling purposes, the dataset was randomly arranged as follows: roughly 80% of the total data (55 observations out of 70) was aimed at training the model, whereas roughly 20% (15 observations out of 70) was aimed at testing it. However, before starting with the training process, two pre-processing procedures were implemented. Min–max normalization was implemented to improve both the convergence time and prediction accuracy of each investigated algorithm. It consisted of scaling each observation to a range between [0, +1] so that the minimum ( $x_{min}$ ) and the maximum ( $x_{max}$ ) values of each variable corresponded to 0 and +1, respectively. The resulting normalized values ( $x_{norm}$ ) were subsequently used for modeling purposes. The mathematical formulation of the min–max normalization procedure is provided in Equation (12).

$$x_{norm} = \frac{x - x_{min}}{x_{max} - x_{min}} \quad (12)$$

K-fold cross-validation (CV) is one of the best-performing strategies for the proper training of a model, and it was implemented here to optimize the investigated algorithms. K-fold CV is an iterative procedure that performs a random partitioning of the training dataset into k different folds. Then, for each of the k iterations, k–1 partitions are used to actually train the model while the remaining one is used to validate it. As a result, k validation scores are obtained, and the model training performance is evaluated as the average of the k-scores. According to well-established bibliographic references, k was assumed to be equal to 5 [60].

To identify the best combination of hyperparameters for each developed model, an extensive grid search was carried out for the several investigated algorithms. Regarding SVMs, the optimized hyperparameters were determined according to the kernel function, namely, C for Lin-SVR, C and  $d$  for Poly-SVR, and C and  $\gamma$  for both RBF-SVR and Sigm-SVR. For CatBoost, three hyperparameters were optimized: the tree maximum depth, the learning rate, and the total number of iterations performed during the training phase. The first one is related to the model architecture, whereas the last two hyperparameters are related to the algorithmic functioning. The corresponding search ranges were identified according to the relevant literature [61] and are summarized in Table 2.

**Table 2.** Search ranges of hyperparameters investigated during the grid search.

ML Model	Feature	Grid	Selected Value
Lin-SVR	C	0.01, 0.1, 1, 10, 100	1
Poly-SVR	C	0.01, 0.1, 1, 10, 100	10
	$d$	2, 3, 4	2
RBF-SVR	C	0.01, 0.1, 1, 10, 100	100
	$\gamma$	0.0001, 0.001, 0.01, 0.1, 1, 10	0.1
Sigm-SVR	C	0.01, 0.1, 1, 10, 100	100
	$\gamma$	0.0001, 0.001, 0.01, 0.1, 1, 10	0.01
CatBoost	Maximum depth	3, 4, 5, 6	3
	Iterations	500, 1000, 5000	1000
	Learning rate	0.005, 0.01, 0.05	0.05

Finally, to prevent the overfitting phenomenon, an overfitting detector was implemented. As the training process proceeded, if the validation scores no longer decreased significantly during subsequent iterations (the threshold was equal to  $10^{-4}$ ), then the training phase was stopped. The number of successive iterations was set at 20, in accordance with the relevant literature [62].

All the pre-processing techniques, the overfitting detection algorithms, and the investigated ML models were developed and implemented in Python 3.9.12.



### 3. Results and Discussion

#### 3.1. Laboratory Results

As shown in Figure 1, for the hot asphalt mixtures involving variable percentages of secondary raw materials, all the alternatives matched the desired target air voids content at the design number of gyrations at 5%, 7.5% and 6.5% TBC, respectively, for HMAmod, HMAc and DW1 and HMAmodC and DW1; the average ITS at 10 °C at 4% SSDV lowered by 15% when using the C and DW1 (HMAmodC and DW1) instead of limestone (HMAmod), while it increased by 47% when using the neat bitumen 50/70 (HMAc and DW1) instead of modified bitumen (HMAmodC and DW1) in combination with the C and DW1.

In general, the cold asphalt mixtures have greater SSDV content and moisture sensitivity, lower ITS and temperature susceptibility compared to hot asphalt mixtures; using secondary raw materials (construction and demolition waste aggregates and filler in any percentage) requires greater optimum water and cement contents to reach the target dry density and allow for proper strength after curing. Nevertheless, the CMAC and DW1 with 4% EBC has, on average, 11% lower ITS compared to CMA, while the mixtures with C and DW2 (CMAC and DW2\_1 with 5% EBC and CMAC and DW2\_2 with 7.5% CC and 5% EBC) have, respectively, 32% and 55% lower ITS compared to CMA.

#### 3.2. Machine Learning Modeling Results

To define the best performing model to accomplish the predictive modeling task, it is important to observe the histogram plot reported in Figure 3 where direct comparisons between target values and the corresponding predictions performed by each model are shown. The above and the bottom diagrams refer to the SSDV and ITS at 10 °C predictions, respectively. On the  $x$ -axis, the IDs of each testing observation used during the testing phase are reported. Conversely, on the  $y$ -axis, black, cyan, orange, gray, purple, and green histograms represent the target values and the predictions made by CatBoost, RBF-SVR, Poly-SVR, Sigm-SVR, and Lin-SVR, respectively. For both SSDV and ITS, it can be observed that the models' predictions do not greatly differ from the target values. This aspect is particularly significant from an engineering point of view, since it confirms that all the developed models make reliable predictions both in terms of SSDV and ITS, thus allowing for a detailed characterization of the analyzed mixtures, both from volumetric and mechanical perspectives. To further evaluate model performance, six goodness-of-fit metrics were considered: mean absolute error (MAE), mean squared error (MSE), root mean squared error (RMSE), mean absolute percentage error (MAPE), Pearson correlation (R), and the determination coefficient ( $R^2$ ). Besides the RMSE described in Equation (1), the mathematical formulation of the other implemented metrics can be expressed as shown in Equations (13)–(17):

$$\text{MAE} = \frac{1}{n} \sum_{i=1}^n |y_{T_i} - y_{P_i}| \quad (13)$$

$$\text{MSE} = \frac{1}{n} \sum_{i=1}^n (y_{T_i} - y_{P_i})^2 \quad (14)$$

$$\text{MAPE} = \frac{1}{n} \sum_{i=1}^n \left| \frac{y_{T_i} - y_{P_i}}{y_{T_i}} \right| \times 100 \quad (15)$$

$$R = \frac{1}{n-1} \sum_{i=1}^n \left( \frac{y_{T_i} - \mu_{y_{T_i}}}{\sigma_{y_{T_i}}} \right) \left( \frac{y_{P_i} - \mu_{y_{P_i}}}{\sigma_{y_{P_i}}} \right) \quad (16)$$

$$R^2 = 1 - \frac{\sum_{i=1}^n (y_{T_i} - y_{P_i})^2}{\sum_{i=1}^n (y_{T_i} - \mu_{y_{T_i}})^2} \quad (17)$$

where  $\mu$  and  $\sigma$  stand for the corresponding mean and the standard deviation, respectively. The results are reported in Table 3.

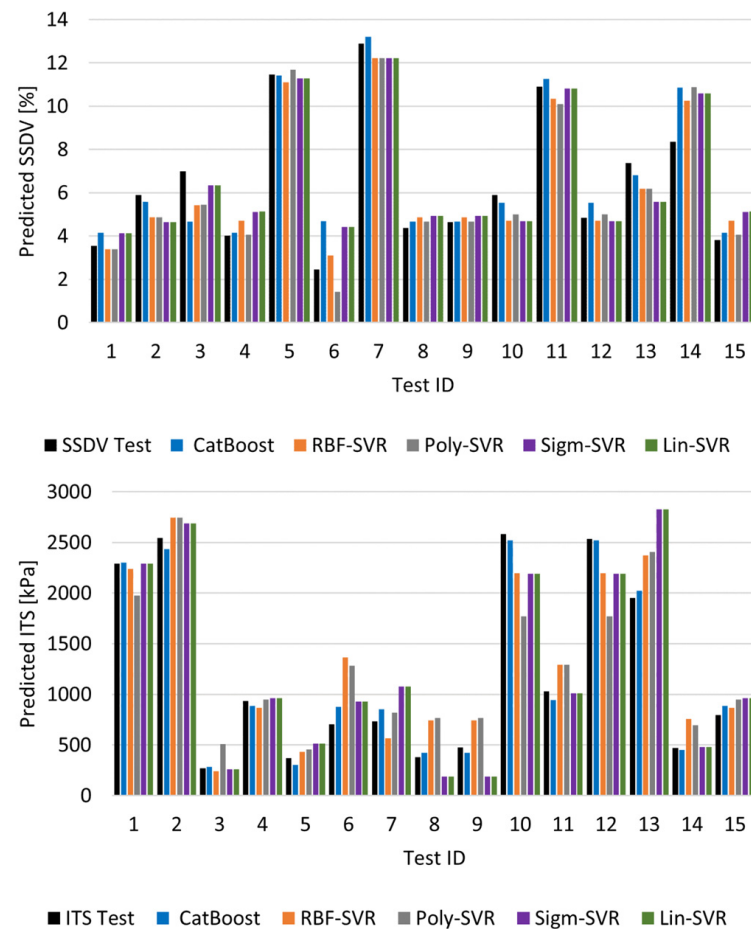


Figure 3. SSDV (up) and ITS (down) histogram plots obtained for each model.

Table 3. Performance metrics evaluation.

ML Model	Performance Metric for SSDV Predictions					
	MAE [%]	MSE [% <sup>2</sup> ]	RMSE [%]	MAPE [%]	R	R <sup>2</sup>
Lin-SVR	0.93	1.31	1.14	19.29	0.9280	0.8591
Poly-SVR	0.72	0.96	0.98	11.93	0.9551	0.8966
RBF-SVR	0.78	0.85	0.92	13.46	0.9541	0.9083
Sigm-SVR	0.93	1.31	1.14	19.27	0.9281	0.8593
CatBoost	0.74	1.23	1.11	15.34	0.9382	0.8678
	Performance Metric for ITS at 10 °C Predictions					
	MAE [kPa]	MSE [kPa <sup>2</sup> ]	RMSE [kPa]	MAPE [%]	R	R <sup>2</sup>
Lin-SVR	212.65	92,854.86	304.72	22.69	0.9425	0.8765
Poly-SVR	325.60	159,005.13	398.75	38.06	0.8991	0.7885
RBF-SVR	243.31	88,112.77	296.84	30.63	0.9478	0.8828
Sigm-SVR	212.66	92,865.59	304.74	22.70	0.9425	0.8765
CatBoost	66.23	6308.81	79.43	8.55	0.9960	0.9916

In terms of SSDV predictions, the performance of all models was fully satisfactory. The results showed MAE values ranging from 0.72% to 0.93%, whereas R<sup>2</sup> values roughly ranged from 0.86 to 0.91, thus demonstrating a balanced performance between the algorithms. In this sense, the investigated ML models returned quite a similar level of reliability. However, the same consideration cannot be made in terms of ITS at 10 °C predictions

because the CatBoost model outperformed the SVR-models, thus returning a higher accuracy. The MAE evaluated with CatBoost predictions were an order of magnitude lower than those returned by the SVR models. Furthermore, CatBoost provided a coefficient of determination equal to 0.99, considerably higher than the value returned, for example, by the Poly-SVR (roughly 0.79).

To further display the predictive performance of the investigated ML models, Figure 4 shows the two regression plots expressed in terms of SSDV predictions on the left and ITS predictions on the right. To remain consistent with the histogram graph, the same colors were used to identify the different models. The  $x$ -axis represents the value of the target observation, while the  $y$ -axis represents the corresponding prediction made by each model. The black solid line inclined at  $45^\circ$  represents the ideal condition of perfect accuracy, in which the observed and predicted values exactly coincide. The closer the diamonds are to this line, the greater the predictive accuracy of the model. Again, it can be observed that, in terms of SSDV, there is substantial equivalence of the different models' predictive performance; conversely, in terms of ITS, it is evident that the CatBoost model achieves remarkable levels of accuracy, outperforming the other SVR models.

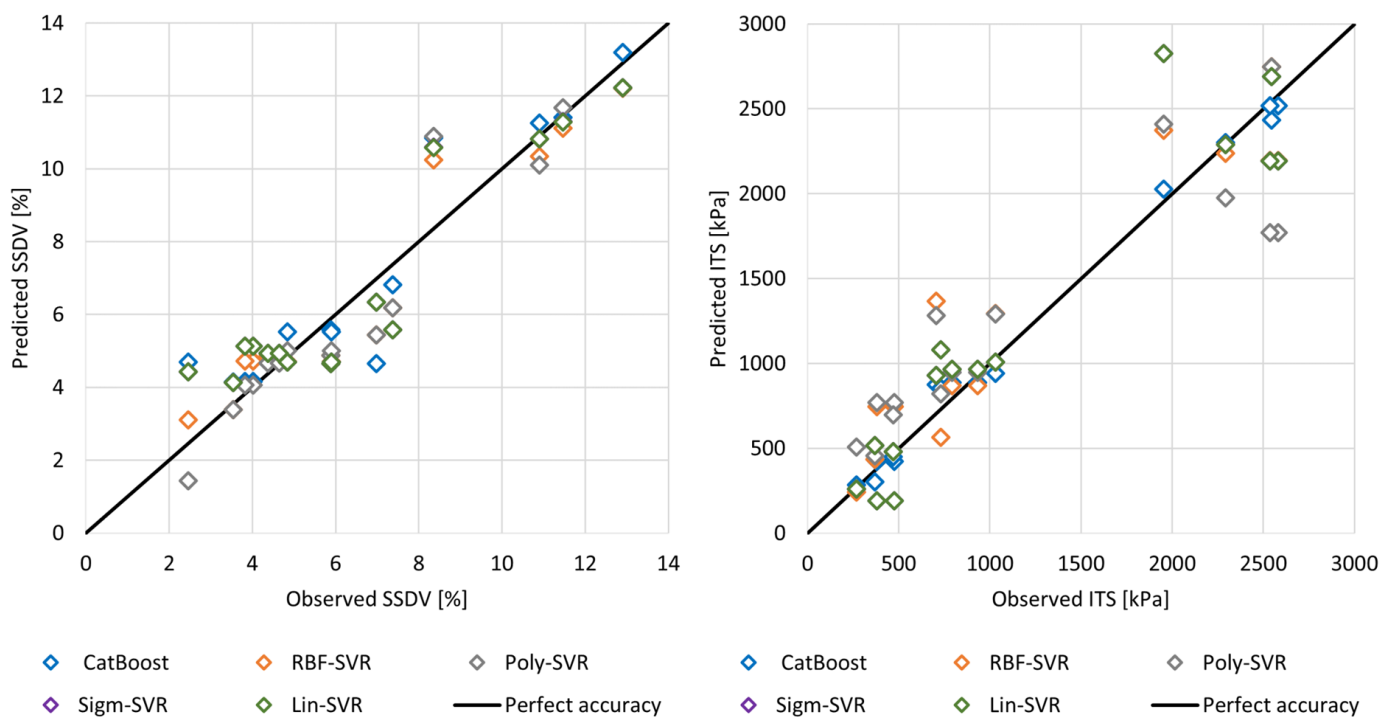


**Figure 4.** SSDV (left) and ITS (right) regression plots obtained for each model.

For this reason, it was decided to focus attention on the CatBoost model, and a sensitivity analysis was performed (Figure 5) to evaluate how much its predictions changed on average if each input feature changed. The cumulative importance of all the different features was set as equal to 100%, and a higher value of importance corresponded to greater variations in the predictions made by the model. Different features were then sorted from top to bottom according to decreasing importance values. As can be observed, RAP (24.67%), WC (21.53%), and the categorical variable (18.56%) represented the three most critical features. These were then followed by EBC (12.30%), TBC (8.91%), and CC (7.05%). Finally, C and DW1 and C and DW2 contents and GR (jointly 6.98%) represented the three less critical features and their importance was comparatively low when volumetric (SSDV) and mechanical (ITS) parameters were predicted.

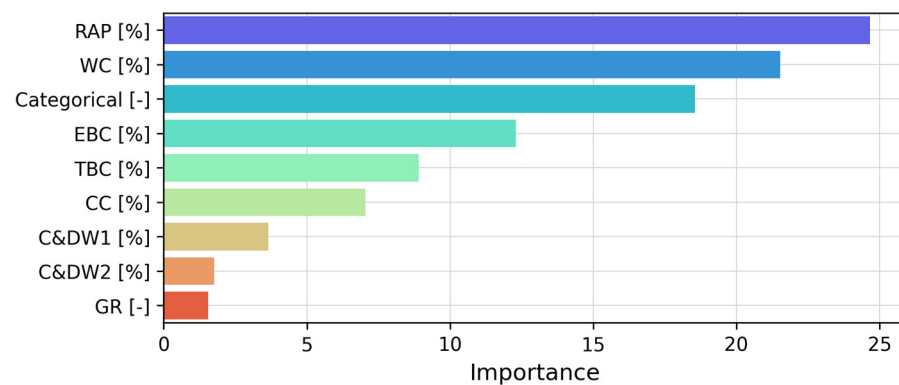


Figure 5. Sensitivity analysis results.

#### 4. Conclusions

During the assessment of the technical suitability of AMs prepared with secondary raw materials, it is essential that the investigated sustainable technological solution matches the threshold values of the road materials' tender specifications, above all the volume of voids and indirect tensile strength. This study aimed to investigate several alternative solutions for the binder course layer of asphalt pavements prepared using different wastes recycled as secondary raw materials as partial replacements for primary materials like limestone aggregates and fillers. Indirect tensile strength tests at 10 °C were carried out to determine the mechanical performance of the mixtures. Subsequently, different ML algorithms (i.e., support vector machines and decision tree-based categorical boosting) were exploited to develop a reliable model for the prediction of the volumetric and mechanical features of the prepared asphalt mixtures. These soft-computing techniques allowed for the obtained laboratory results to be processed in order to train, validate and subsequently test the designed predictive methodologies. Six goodness-of-fit metrics were evaluated to fully describe the performance achieved by each model. Based on the obtained findings, the following conclusions were drawn:

- The experimental laboratory phase consisted of the identification of the optimum bitumen content, in the case of hot asphalt mixtures, to reach the target air voids content of 4% by varying the content of construction and demolition waste aggregates and the bitumen type (i.e., neat and SBS-modified bitumen); independently from the percentage content of construction and demolition waste aggregates and from the bitumen type, all the alternative mixtures required a higher optimum bitumen content compared to the traditional one. Similarly, the optimum composition of cold asphalt mixtures with construction and demolition waste that minimizes the volume of voids often matched higher cement and water demand compared to the traditional cold mix asphalt, apparently showing a significantly lower ITS when substituting the limestone filler with the recycled filler;
- The extensive grid search allowed for the best hyperparameters to be properly identified with respect to each investigated soft-computing technique, returning remarkable predictive performances;
- Based on a categorical variable identifying the mixing technology, the number of gyratory revolutions, and the percentage contents of RAP, water, emulsion bitumen, total bitumen, cement, and construction and demolition wastes, both the SVR and CatBoost models were capable of properly predicting SSDV, with similar  $R^2$  values ranging from 0.86 to 0.91;
- CatBoost outperformed the SVR models in terms of ITS predictions, achieving a coefficient of determination of  $R^2$  equal to 0.99. This was significantly higher than those obtained evaluating different SVR model predictions since the second-highest value resulted from RBF-SVR and was roughly equal to 0.88. The lowest  $R^2$  score was obtained by the Poly-SVR (roughly 0.79);

- A sensitivity analysis was carried out to identify the features that most influenced CatBoost predictions of SSDV and ITS. The results highlighted that RAP percentage content was the most critical feature (with a normalized importance of 24.67%), followed by WC (21.53%), and the categorical variable (18.56%). Conversely, the importance of C and DW contents and GR was comparatively low;
- With respect to the experimental study, current shortcomings are related to the lack of fatigue life and/or permanent deformation resistance investigations. On the other hand, with respect to the predictive modeling, the developed methodology has a limitation in its validation since it was developed to be applied to all mixture types, but it was actually only validated based on the investigated types. Furthermore, other machine learning algorithms, namely, artificial neural networks, could be adopted to model such volumetric and mechanical properties, and other regression techniques could be used for direct comparisons. However, the results obtained from both the laboratory analyses and predictive modeling using the CatBoost algorithm were very promising. This strongly encourages future developments in several areas such as: (i) the study of mixtures prepared with higher percentages of recycled materials to achieve increasingly higher standards of circularity and environmental sustainability; (ii) the prediction of the dynamic behavior of the asphalt mixtures in terms of the stiffness modulus, resistance to fatigue cracking, and accumulation of ruts; and (iii) the search for increasingly advanced and innovative machine learning algorithms in order to make predictive modeling even more accurate and reliable.

**Author Contributions:** Conceptualization, F.A. and N.B.; methodology, F.R., C.O., F.A. and N.B.; software, F.R.; validation, F.R., C.O., F.A. and N.B.; formal analysis, F.R. and C.O.; investigation, C.O. and F.A.; resources, F.A. and N.B.; data curation, F.R., C.O. and F.A.; writing—original draft preparation, F.R., C.O., F.A. and N.B.; writing—review and editing, F.R., C.O., F.A. and N.B.; visualization, F.R., C.O., F.A. and N.B.; supervision, N.B.; project administration, F.A. and N.B.; funding acquisition, F.A. and N.B. All authors have read and agreed to the published version of the manuscript.

**Funding:** This research received no external funding.

**Institutional Review Board Statement:** Not applicable.

**Informed Consent Statement:** Not applicable.

**Data Availability Statement:** The data that support the findings of this study are available from the corresponding author upon reasonable request.

**Conflicts of Interest:** The authors declare no conflict of interest.

## References

1. Subramaniam, N.; Akbar, S.; Situ, H.; Ji, S.; Parikh, N. Sustainable development goal reporting: Contrasting effects of institutional and organisational factors. *J. Clean. Prod.* **2023**, *411*, 137339. [[CrossRef](#)]
2. Lee, B.X.; Kjaerulf, F.; Turner, S.; Cohen, L.; Donnelly, P.D.; Muggah, R.; Davis, R.; Realini, A.; Kieselbach, B.; MacGregor, L.S.; et al. Transforming Our World: Implementing the 2030 Agenda Through Sustainable Development Goal Indicators. *J. Public Health Pol.* **2016**, *37*, 13–31. [[CrossRef](#)] [[PubMed](#)]
3. Senadjki, A.; Awal, I.M.; Nee, A.Y.H.; Ogbeibu, S. The belt and road initiative (BRI): A mechanism to achieve the ninth sustainable development goal (SDG). *J. Clean. Prod.* **2022**, *372*, 133590. [[CrossRef](#)]
4. Huang, Y.; Shafiee, M.; Charnley, F.; Encinas-Oropesa, A. Designing a Framework for Materials Flow by Integrating Circular Economy Principles with End-of-Life Management Strategies. *Sustainability* **2022**, *14*, 4244. [[CrossRef](#)]
5. Khajuria, A.; Atienza, V.A.; Chavanich, S.; Henning, W.; Islam, I.; Kral, U.; Liu, M.; Liu, X.; Murthy, I.K.; Oyedotun, T.D.T.; et al. Accelerating circular economy solutions to achieve the 2030 agenda for sustainable development goals. *Circ. Econ.* **2022**, *1*, 100001. [[CrossRef](#)]
6. Li, Z.; Guo, T.; Chen, Y.; Zhao, X.; Chen, Y.; Yang, X.; Wang, J. Road performance analysis of cement stabilized coal gangue mixture. *Mater. Res. Express* **2021**, *8*, 125502. [[CrossRef](#)]
7. Cai, Y.; Liu, X. Mechanical properties test of pavement base or subbase made of solid waste stabilized by acetylene sludge and fly ash. *AIP Adv.* **2020**, *10*, 065022. [[CrossRef](#)]
8. Behera, B.; Mishra, M.K. Strength behaviour of surface coal mine overburden–fly ash mixes stabilised with quick lime. *Int. J. Min. Reclam. Environ.* **2012**, *26*, 38–54. [[CrossRef](#)]

9. Wu, S.; Montalvo, L. Repurposing waste plastics into cleaner asphalt pavement materials: A critical literature review. *J. Clean. Prod.* **2021**, *280*, 124355. [[CrossRef](#)]
10. Zhao, W.; Yang, Q. Design and performance evaluation of a new green pavement: 100% recycled asphalt pavement and 100% industrial solid waste. *J. Clean. Prod.* **2023**, *421*, 138483. [[CrossRef](#)]
11. Abreu, L.P.; Oliveira, J.R.; Silva, H.M.; Fonseca, P.V. Recycled asphalt mixtures produced with high percentage of different waste materials. *Constr. Build. Mater.* **2015**, *84*, 230–238. [[CrossRef](#)]
12. Baldo, N.; Rondinella, F.; Daneluz, F.; Pasetto, M. Foamed Bitumen Mixtures for Road Construction Made with 100% Waste Materials: A Laboratory Study. *Sustainability* **2022**, *14*, 6056. [[CrossRef](#)]
13. Abed, A.H.; Bahia, H.U. Enhancement of permanent deformation resistance of modified asphalt concrete mixtures with nano-high density polyethylene. *Constr. Build. Mater.* **2020**, *236*, 117604. [[CrossRef](#)]
14. Nouali, M.; Derriche, Z.; Ghorbel, E.; Li, C. Plastic bag waste modified bitumen a possible solution to the Algerian road pavements. *Road Mater. Pavement Des.* **2020**, *21*, 1713–1725. [[CrossRef](#)]
15. Dalhat, M.A.; Al-Abdul Wahhab, H.I. Performance of recycled plastic waste modified asphalt binder in Saudi Arabia. *Int. J. Pavement Eng.* **2017**, *18*, 349–357. [[CrossRef](#)]
16. Romano, G.; Rapposelli, A.; Marrucci, L. Improving waste production and recycling through zero-waste strategy and privatization: An empirical investigation. *Resour. Conserv. Recycl.* **2019**, *146*, 256–263. [[CrossRef](#)]
17. Pasetto, M.; Baldo, N. Cement bound mixtures with metallurgical slags for road constructions: Mix design and mechanical characterization. *IM Inž. Miner.* **2013**, *14*, 15–20.
18. Di Benedetto, H.; Olard, F.; Sauzéat, C.; Delaporte, B. Linear viscoelastic behaviour of bituminous materials: From binders to mixes. *Road Mater. Pavement Des.* **2004**, *5*, 163–202. [[CrossRef](#)]
19. Ceylan, H.; Gopalakrishnan, K.; Kim, S. Advanced approaches to hot-mix asphalt dynamic modulus prediction. *Can. J. Civ. Eng.* **2008**, *35*, 699–707. [[CrossRef](#)]
20. Sakhaeifar, M.S.; Kim, Y.R.; Kabir, P. New predictive models for the dynamic modulus of hot mix asphalt. *Constr. Build. Mater.* **2015**, *76*, 221–231. [[CrossRef](#)]
21. Cao, P.; Jin, F.; Feng, D.; Zhou, C.; Hu, W. Prediction on dynamic modulus of asphalt concrete with random aggregate modeling methods and virtual physics engine. *Constr. Build. Mater.* **2016**, *125*, 987–997. [[CrossRef](#)]
22. Nemati, R.; Dave, E.V. Nominal property based predictive models for asphalt mixture complex modulus (dynamic modulus and phase angle). *Constr. Build. Mater.* **2018**, *158*, 308–319. [[CrossRef](#)]
23. Bari, J. Development of a New Revised Version of the Witczak E\* Predictive Models for Hot Mix Asphalt Mixtures. Doctoral Dissertation, Arizona State University, Phoenix, AZ, USA, 2005.
24. Witczak, M.; El-Basyouny, M.; El-Badawy, S. *Incorporation of the New (2005) E\* Predictive Model in the MEPDG*; NCHRP 1-40D Final Report; Arizona State University: Tempe, AZ, USA, 2007.
25. Giunta, M.; Pisano, A.A. One dimensional viscoelastoplastic constitutive model for asphalt concrete. *Multidiscip. Model. Mater. Struct.* **2006**, *2*, 247–264. [[CrossRef](#)]
26. Pasetto, M.; Baldo, N. Computational analysis of the creep behaviour of bituminous mixtures. *Constr. Build. Mater.* **2015**, *94*, 784–790. [[CrossRef](#)]
27. Baldo, N.; Miani, M.; Rondinella, F.; Manthos, E.; Valentin, J. Road Pavement Asphalt Concretes for Thin Wearing Layers: A Machine Learning Approach towards Stiffness Modulus and Volumetric Properties Prediction. *Period. Polytech. Civ. Eng.* **2022**, *66*, 1087–1097. [[CrossRef](#)]
28. Phung, B.N.; Le, T.H.; Nguyen, T.A.; Hoang, H.G.T.; Ly, H.B. Novel approaches to predict the Marshall parameters of basalt fiber asphalt concrete. *Constr. Build. Mater.* **2023**, *400*, 132847. [[CrossRef](#)]
29. Majidifard, H.; Jahangiri, B.; Buttler, W.G.; Alavi, A.H. New machine learning-based prediction models for fracture energy of asphalt mixtures. *Measurement* **2019**, *135*, 438–451. [[CrossRef](#)]
30. Ghafari, S.; Ehsani, M.; Nejad, F.M. Prediction of low-temperature fracture resistance curves of unmodified and crumb rubber modified hot mix asphalt mixtures using a machine learning approach. *Constr. Build. Mater.* **2022**, *314*, 125332. [[CrossRef](#)]
31. Specht, L.P.; Khatchaturian, O.; Brito, L.A.T.; Ceratti, J.A.P. Modeling of asphalt-rubber rotational viscosity by statistical analysis and neural networks. *Mater. Res.* **2007**, *10*, 69–74. [[CrossRef](#)]
32. Mirzahosseini, M.R.; Aghaeifar, A.; Alavi, A.H.; Gandomi, A.H.; Seyednour, R. Permanent deformation analysis of asphalt mixtures using soft computing techniques. *Expert Syst. Appl.* **2011**, *38*, 6081–6100. [[CrossRef](#)]
33. Androjić, I.; Marović, I. Development of artificial neural network and multiple linear regression models in the prediction process of the hot mix asphalt properties. *Can. J. Civ. Eng.* **2017**, *44*, 994–1004. [[CrossRef](#)]
34. Alrashydah, E.I.; Abo-Qudais, S.A. Modeling of creep compliance behavior in asphalt mixes using multiple regression and artificial neural networks. *Constr. Build. Mater.* **2018**, *159*, 635–641. [[CrossRef](#)]
35. Ziari, H.; Amini, A.; Goli, A.; Mirzaiyan, D. Predicting rutting performance of carbon nano tube (CNT) asphalt binders using regression models and neural networks. *Constr. Build. Mater.* **2018**, *160*, 415–426. [[CrossRef](#)]
36. Barugahare, J.; Amirkhanian, A.N.; Xiao, F.; Amirkhanian, S.N. Predicting the dynamic modulus of hot mix asphalt mixtures using bagged trees ensemble. *Constr. Build. Mater.* **2020**, *260*, 120468. [[CrossRef](#)]
37. Vapnik, V. *The Nature of Statistical Learning Theory*; Springer: Berlin/Heidelberg, Germany, 1995; ISBN 0-387-94559-8.

38. Liu, J.; Liu, F.; Zheng, C.; Fanijo, E.O.; Wang, L. Improving asphalt mix design considering international roughness index of asphalt pavement predicted using autoencoders and machine learning. *Constr. Build. Mater.* **2022**, *360*, 129439. [[CrossRef](#)]
39. Yang, E.; Yang, Q.; Li, J.; Zhang, H.; Di, H.; Qiu, Y. Establishment of icing prediction model of asphalt pavement based on support vector regression algorithm and Bayesian optimization. *Constr. Build. Mater.* **2022**, *351*, 128955. [[CrossRef](#)]
40. Ke, G.; Meng, Q.; Finley, T.; Wang, T.; Chen, W.; Ma, W.; Ye, Q.; Liu, T.Y. Lightgbm: A highly efficient gradient boosting decision tree. In Proceedings of the Advances in Neural Information Processing Systems, Long Beach, CA, USA, 4–9 December 2017; pp. 3147–3155.
41. Chen, T.; Guestrin, C. Xgboost: A scalable tree boosting system. *arXiv* **2016**, arXiv:1603.02754. [[CrossRef](#)]
42. Prokhorenkova, L.; Gusev, G.; Vorobev, A.; Dorogush, A.V.; Gulin, A. CatBoost: Unbiased boosting with categorical features. *arXiv* **2017**, arXiv:1706.09516. [[CrossRef](#)]
43. Nguyen, H.L.; Tran, V.Q. Data-driven approach for investigating and predicting rutting depth of asphalt concrete containing reclaimed asphalt pavement. *Constr. Build. Mater.* **2023**, *377*, 131116. [[CrossRef](#)]
44. UNI EN 13108-8:2016; Bituminous Mixtures—Material Specifications—Part 8: Reclaimed Asphalt. European Committee for Standardization: Brussels, Belgium, 2016.
45. Azienda Nazionale Autonoma delle Strade. *Capitolato Speciale D'appalto—Norme Tecniche*; Azienda Nazionale Autonoma delle Strade: Roma, Italy, 2021. (In Italian)
46. UNI EN 1097-2:2020; Tests for Mechanical and Physical Properties of Aggregates—Part 2: Methods for the Determination of Resistance to Fragmentation. European Committee for Standardization: Brussels, Belgium, 2020.
47. UNI EN 933-3:2012; Tests for Geometrical Properties of Aggregates—Part 3: Determination of Particle Shape—Flakiness Index. European Committee for Standardization: Brussels, Belgium, 2012.
48. UNI EN 933-8:2012+A1:2015; Tests for Geometrical Properties of Aggregates—Part 8: Assessment of Fines—Sand Equivalent Test. European Committee for Standardization: Brussels, Belgium, 2015.
49. EN 12697-6: 2020; Bituminous Mixtures—Test Methods—Part 6: Determination of Bulk Density of Bituminous Specimens. European Committee for Standardization: Brussels, Belgium, 2020.
50. EN 12697-8: 2019; Bituminous Mixtures—Test Methods—Part 8: Determination of Void Characteristics of Bituminous Specimens. European Committee for Standardization: Brussels, Belgium, 2019.
51. EN 12697-23: 2018; Bituminous Mixtures—Test Methods—Part 23: Determination of the Indirect Tensile Strength of Bituminous Specimens. European Committee for Standardization: Brussels, Belgium, 2018.
52. Cortes, C.; Vapnik, V. Support-vector networks. *Mach. Learn.* **1995**, *20*, 273–297. [[CrossRef](#)]
53. Babagoli, R.; Rezaei, M. Prediction of moisture resistance of asphalt mastics modified by liquid anti stripping based on support vector regression, artificial neural network and Kernel-based support vector regression methods. *Constr. Build. Mater.* **2022**, *335*, 127480. [[CrossRef](#)]
54. Kutateladze, V. The kernel trick for nonlinear factor modeling. *Int. J. Forecast.* **2022**, *38*, 165–177. [[CrossRef](#)]
55. Kearns, M.; Valiant, L. Cryptographic limitations on learning boolean formulae and finite automata. *J. ACM* **1994**, *41*, 67–95. [[CrossRef](#)]
56. Ferov, M.; Modrý, M. Enhancing lambdamart using oblivious trees. *arXiv* **2016**, arXiv:1609.05610. [[CrossRef](#)]
57. Gulin, A.; Kuralenok, I.; Pavlov, D. Winning the transfer learning track of yahoo!'s learning to rank challenge with yetirank. In Proceedings of the Learning to Rank Challenge, Haifa, Israel, 25 June 2011.
58. Lou, Y.; Obukhov, M. Bdt: Gradient boosted decision tables for high accuracy and scoring efficiency. In Proceedings of the 23rd ACM SIGKDD International Conference on Knowledge Discovery and Data Mining, Halifax, NS, Canada, 13–17 August 2017. [[CrossRef](#)]
59. Lee, S.; Vo, T.P.; Thai, H.T.; Lee, J.; Patel, V. Strength prediction of concrete-filled steel tubular columns using Categorical Gradient Boosting algorithm. *Eng. Struct.* **2021**, *238*, 112109. [[CrossRef](#)]
60. Kuhn, M.; Johnson, J. *Applied Predictive Modeling*; Springer: New York, NY, USA, 2013. [[CrossRef](#)]
61. Beniwal, M.; Singh, A.; Kumar, N. Forecasting long-term stock prices of global indices: A forward-validating Genetic Algorithm optimization approach for Support Vector Regression. *Appl. Soft Comput.* **2023**, *145*, 110566. [[CrossRef](#)]
62. James, G.; Witten, D.; Hastie, T.; Tibshirani, R. *An Introduction to Statistical Learning with Applications in R.*; Springer: New York, NY, USA, 2013. [[CrossRef](#)]

**Disclaimer/Publisher's Note:** The statements, opinions and data contained in all publications are solely those of the individual author(s) and contributor(s) and not of MDPI and/or the editor(s). MDPI and/or the editor(s) disclaim responsibility for any injury to people or property resulting from any ideas, methods, instructions or products referred to in the content.